Received: 29 January 2024 | Revised: 13 October 2024 | Accepted: 22 October 2024

IET Communications

DOI: 10.1049/cmu2.12858

The Institution of Engineering and Technology WILEY

ORIGINAL RESEARCH

Analysis of error rates and capacity outage of wireless links under jamming and multipath signal fading

Jan Mietzner

Hamburg University of Applied Sciences, Faculty of Design, Media, and Information, Research & Transfer Center Digital Reality, Hamburg, Germany

Correspondence
Jan Mietzner, Hamburg University of Applied Sciences, Faculty of Design, Media, and Information, Research, and Transfer Center Digital Reality, D-22081 Hamburg, Germany.
Email: jan.mietzner@haw-hamburg.de

Abstract

The author addresses the question, under which conditions an active jammer will be successful in corrupting a wireless communication link, when both the desired link and the jamming link are subject to multipath signal fading. To this end, a simple closed-form analytical expression is derived for the resulting block-error probability (BLEP) under Nakagami-*m* fading with in general unequal fading parameters for the desired and the jamming link. As a by-product, a novel expression for the corresponding probability of a capacity outage is obtained. An asymptotic analysis and numerical evaluation of the BLEP expression show that in the single-antenna case the jammer will indeed be successful in corrupting the wireless link, unless there is a rather high signal-to-noise ratio (SNR) advantage for the desired link. This even holds true, when signal fading for the jamming link is significantly more severe than for the desired link. Finally, the case of multiple antennas is considered and the benefits of array processing and diversity reception at the desired receiver are explored. It is found that receive array processing can significantly improve the resulting BLEP, provided that the desired link is characterized by favorable fading conditions. On the other hand, diversity reception can significantly improve the BLEP, if the desired link has favorable SNR conditions.

1 | INTRODUCTION

Performance prediction for wireless communications—based on analytical results or corresponding (Monte-Carlo) computer simulations—is important, in order to ensure that practical systems eventually meet expected quality-of-service parameters. In fact, the influence of interference tends to play an increasingly dominant role, given that fifth-generation mobile radio systems will witness user densities that are far higher than in legacy fourth-generation systems [1].

In this paper, we look at the special case of active jamming as an example of *intentional* interference. In particular, we address the question, under which conditions the jammer will be successful in corrupting a wireless communication link, when both the desired link and the jamming link are subject to multipath signal fading. Interference scenarios over (non-fading) additive-white-Gaussian-noise (AWGN) channels with a larger number of (unintentional) interferers are often modeled by employing a Gaussian approximation for the resulting sum interference signal. However, scenarios involving a single active jammer in the vicinity of a desired receiver are usually not well captured by a Gaussian interference model. Furthermore, considering multipath signal fading on the desired and the interfering link(s) adds additional complexity to performance analysis.

Various papers have addressed specific scenarios with a single or multiple dominant interferers or jammers in the presence of multipath signal fading. For example, the authors of [2] considered Rician and Nakagami-*m* multipath fading for the desired link, while the interference links were assumed to be subject to Rayleigh fading and were represented by a Gaussian model. Scenarios with Rayleigh or Rician fading for both the desired link and the interfering link(s) were, for example, addressed in [3]. A scenario with two dominant interference links subject to Rayleigh fading was considered in [4], where the desired link was assumed to be characterized by Nakagami-*m* fading.

The case of multiple receive antennas with optimum combining at the desired receiver was analyzed in [5] for the case when both the desired and the interfering links are subject to Rayleigh fading. Equal-gain combining for a combination of

Nakagami-m fading on the desired links and Rayleigh fading on the interfering links was investigated in [6]. Maximum-ratio combining (MRC) at the desired receiver was considered in [7], where both the desired and the interfering links were assumed to be subject to Nakagami-m fading. AWGN at the receiver was disregarded for simplicity, however. In [8], focus was on amplify-and-forward relaying with Nakagami-m fading on the source-relay and the relay-destination link as well as on the interfering links. More general fading models for point-to-point links—both for the desired and the interfering links—were investigated in [9].

More specifically, for the case of multiple receive antennas and MRC at the desired receiver, multiple interfering links and Nakagami-m fading for all links with in general unequal fading parameters, analytical expressions for the resulting outage probability of the desired link were derived in [10–12]. In particular, [10, 11] looked at general non-integer fading parameters m and devised analytical expressions, which need to be evaluated using numerical integration methods. Additionally, the authors of [11] looked at the special cases of high interference powers and integer-valued fading parameters m and derived corresponding closed-form analytical expressions for both cases. Furthermore, a unified moment-based approach, which also yields closed-form expressions for the case of integer-valued fading parameters m, can be found in [12].

While the closed-form expressions in [11, 12] are quite general, the simple—yet important—special case of a single dominant interferer or active jammer has not been analyzed in detail. In particular, it is interesting to study the impact and interplay of the average signal-to-noise ratios (SNRs) and fading parameters of the desired and the jamming link(s). By this means, it is possible to identify cases, in which the desired link is effectively corrupted or—vice versa—remains widely unaffected. In this context, the Nakagami-m fading model is very attractive, since it provides a fairly general and versatile framework.

More recent publications do also not address these basic questions in detail, but rather investigate more general aspects, such as jammer suppression in wireless communication systems with massive antenna arrays [13, 14], cooperative jamming in fading environments for covert communication [15], cooperative jamming in non-orthogonal multiple-access relaying networks under Rayleigh-fading conditions [16], energy-harvesting jamming under Rayleigh fading conditions with special focus on bursty data traffic [17], or the use of intelligent reflecting surfaces for passive jamming attacks based on induced channel aging [18].

As can be seen, investigations on multipath fading channel modeling with coincidental or intentional interference have a longer tradition in the literature and somewhat peaked in the years 2007–2017 [2] – [12]. Afterwards, efforts were focused on extending the basic system model in various directions [13] – [18], rather than to revisit the basic model and address further modeling aspects in detail.

In order to deepen the knowledge in the available literature and to close identified gaps regarding the basic model, we make the following main contributions:

- For the single-antenna case, we derive a simple closed-form analytical expression for the resulting outage probability of the desired link in the case of Nakagami-m fading with in general different SNR and fading parameters for the desired link and the jamming link. Assuming quasi-static block-fading channel conditions, the outage probability is equivalent to the resulting block-error probability (BLEP) of the desired link. We basically follow the derivation presented in [11], but derive the outage probability for the case of a single dominant interferer/ active jammer from scratch. We thus arrive at an expression for integer-valued Nakagami fading parameters, which is included in equation (18) of [11] as a special case. Yet, the simple structure of our analytical expression yields additional insights regarding the interplay of the average link SNRs and fading parameters for the considered special case of a single interferer/ jammer, which are not readily deduced from the general expression in [11].
- We show that the BLEP tends to one when the average SNR of the jamming link (called jammer-to-noise ratio, JNR, in the sequel) tends to infinity. Moreover, this asymptotic value is approached faster, when the fading parameter of the jamming link has a large value, representing light fading conditions. Yet, numerical evaluation shows that this effect is less significant and that the average JNR turns out to be the key parameter for successful corruption of the desired link. As a bottom line, the jammer will be able to successfully corrupt the desired link, unless there is a rather high SNR advantage for the desired link—even if signal fading for the jamming link is more severe than for the desired link (represented by a small Nakagami fading parameter for the jammer).
- As a by-product, we obtain a corresponding expression for the probability of a capacity outage, which is novel to the best of knowledge. So far, only the probability density function (PDF) of the instantaneous capacity of the desired link has been derived for the considered scenario, and it only applies for the special case of a strong jammer/ interferer [19].
- Finally, we consider the case of multiple antennas and explore the benefits of array processing and diversity reception at the desired receiver. Regarding diversity reception, in the available literature [7, 11] it is usually assumed that the interfering/ jamming signal is identical for all diversity branches, that is, fully correlated, whereas for the desired signal uncorrelated fading is assumed. We extend this model to uncorrelated fading for the jamming signal and assess the resulting performance differences compared to the fully correlated model. We find that diversity reception at the desired receiver can significantly improve the resulting BLEP, provided that the desired link is characterized by rather favorable SNR conditions. On the other hand, array processing at the desired receiver can significantly improve the resulting BLEP, provided that the desired link is characterized by rather favorable fading conditions.

With the above contributions, we complement the available literature on multipath fading channel modeling with (intentional) interference and provide corresponding tools to analyze basic scenarios in more detail.

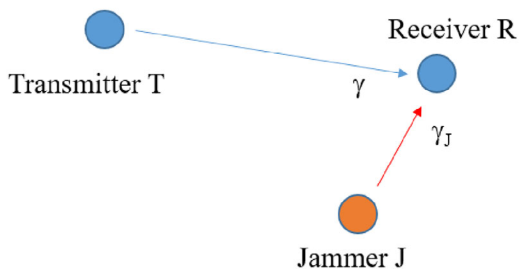

FIGURE 1 Jamming scenario under consideration.

1.1 | Paper organization

The paper is organized as follows: In Section 2, the system model under consideration is introduced, and in Section 3 the analysis of the BLEP resulting for the desired link is presented along with corresponding asymptotic considerations. Numerical performance examples are provided in Section 4, complemented by Monte-Carlo computer simulation results. The case of multiple antennas at the jammer and the desired receiver is discussed in Section 5. Finally, conclusions are drawn in Section 6, and possible directions for future work are pointed out.

Notation 1. Throughout, $\Pr\{\mathcal{E}\}$ denotes the probability of an event $\mathcal{E}$ and $\mathrm{E}\{.\}$ denotes statistical expectation. Moreover, $\bar{x} := \mathrm{E}\{x\}$ denotes the mean value of a random variable x, and $p(x)$ and $C(x)$ denote the corresponding PDF and cumulative distribution function (CDF), respectively. Finally, $(.)^*$ represents complex conjugation.

2 | SYSTEM MODEL

Throughout this paper, we make use of the equivalent complex baseband notation. We consider a wireless link from a transmitter (T) to a desired receiver (R), as shown in Figure 1, which is assumed to be characterized by multipath signal fading conditions according to a Nakagami model with fading parameter $m \in [0.5, \infty)$. Moreover, an active jammer (J) is found in the vicinity, which sends out an (intentional) interference signal in the direction of the desired receiver R. The interference signal observed at the desired receiver R is also assumed to be characterized by Nakagami fading with an in general different fading parameter $m_J \in [0.5, \infty)$ $(m_J \neq m)$. In the following, all nodes (T, R, J) are assumed to be equipped with a single antenna. Possible extensions to multiple-antenna settings will be discussed in Section 5. Furthermore, the desired link is assumed to employ a fixed frequency band with a bandwidth of B Hz.[1] Assuming frequency non-selective channel conditions (or a suitable multi-carrier transmission scheme), the instantaneous signal-to-interference-plus-noise ratio (SINR) at the desired receiver R is given by

$$\rho = \frac{\gamma}{\gamma_J + 1}, \tag{1}$$

where $\gamma := P|h|^2/\sigma^2$ denotes the instantaneous SNR of the desired link T → R, P denotes the average transmit power of transmitter T, h denotes the complex-valued channel coefficient of the desired link, and σ^2 denotes the variance of the AWGN at the desired receiver, which is assumed to be complex-valued and circularly-symmetric Gaussian distributed with mean zero. Similarly, $\gamma_J := P_J|h_J|^2/\sigma^2$ denotes the instantaneous JNR at the desired receiver R, P_J denotes the average transmit power of jammer J, and h_J denotes the complex-valued channel coefficient of the jamming link J → R. Throughout, we assume that quasi-static fading conditions are prevalent, that is, the channel coefficients h and h_J remain approximately constant throughout the transmission of a single data block and change randomly from one data block to the next.[2] In order to keep our analysis general (and independent of any specific channel coding scheme), we assume that some threshold SINR value is given, denoted as ρ_0 in the sequel, which is required (and sufficient) for successful channel decoding. Hence, as long as the instantaneous SINR ρ is larger than the threshold value ρ_0, data blocks are assumed to be decoded correctly at the desired receiver $(\rho > \rho_0)$. Otherwise, decoding is not successful and block errors occur $(\rho \le \rho_0)$. In the following section, we derive a closed-form expression for the resulting outage probability of the desired link as a function of threshold parameter ρ_0 for integer-valued Nakagami fading parameters m and m_J. Under the above assumptions, the outage probability is equivalent to the resulting BLEP of the desired link.

3 | ANALYSIS OF BLOCK ERROR PROBABILITY AND OUTAGE PROBABILITY

Following the assumptions detailed in Section 2, the resulting BLEP is given by

$$P_{BLEP,\rho_0} = C(\rho_0), \tag{2}$$

where $C(\rho)$ denotes the CDF of the instantaneous SINR ρ, and ρ_0 denotes the required SINR at the receiver for successful decoding. Correspondingly, the BLEP may be evaluated as follows:

$$\begin{aligned} P_{BLEP,\rho_0} &= \Pr\{\rho \le \rho_0\} \\ &= \Pr\big\{\gamma \le \rho_0(\gamma_J + 1)\big\}. \end{aligned} \tag{3}$$

[1] The results presented in the sequel will, generally, also hold when a frequency-hopping scheme is employed for the desired link, provided that the multipath fading is still characterized by Nakagami-m/m_J fading and the jammer is able to follow the employed hopping pattern.

[2] In the case of fast fading, the error performance will usually degrade due to outdated channel state information at the receiver. Yet, the BLEP results presented in the sequel may still serve as lower performance limits.

Thus, we have

$$P_{BLEP,\rho_0} = \int_0^\infty p(\gamma_J) \underbrace{\int_0^{\rho_0(\gamma_J+1)} p(\gamma)\,\mathrm{d}\gamma}_{=:I_0}\ \mathrm{d}\gamma_J. \tag{4}$$

Since the desired link T → R is assumed to be subject to Nakagami fading with fading parameter $m \in [0.5, \infty)$, the PDF of γ is given by [20]

$$p(\gamma) = \frac{m^m \gamma^{m-1}}{\bar{\gamma}^m \Gamma(m)}\ \mathrm{e}^{-m\gamma/\bar{\gamma}} \tag{5}$$

($\gamma > 0$), where $\bar{\gamma} := \mathrm{E}\{\gamma\}$ denotes the average SNR of the desired link T → R, and

$$\Gamma(x) = \int_0^\infty \xi^{x-1}\ \mathrm{e}^{-\xi}\ \mathrm{d}\xi \tag{6}$$

denotes the Gamma function [21, §8.310, no. 1]. The special case of $m = 1$ corresponds to the case of Rayleigh fading, whereas $m > 1$ models cases of lighter fading conditions compared to Rayleigh fading, corresponding to a lower probability of small instantaneous SNR values γ. Moreover, the case $m \to \infty$ corresponds to a non-fading line-of-sight link. For simplicity, we focus on the case of a single receive antenna in the sequel ($N = 1$). Possible extensions to multiple-antenna settings will be discussed in Section 5. Based on (5), the integral I_0 in (4) results as

$$I_0 = 1\ -\ \frac{m^m}{\bar{\gamma}^m\Gamma(m)} \int_{\rho_0(\gamma_J+1)}^\infty \gamma^{m-1}\ \mathrm{e}^{-m\gamma/\bar{\gamma}}\ \mathrm{d}\gamma. \tag{7}$$

Substituting $z := \gamma - \rho_0(\gamma_J + 1)$ yields

$$I_0 = 1 - \frac{m^m}{\bar{\gamma}^m\Gamma(m)}\ \mathrm{e}^{-m\rho_0(\gamma_J+1)/\bar{\gamma}} \times \\ \times \int_0^\infty (z + \rho_0(\gamma_J+1))^{m-1}\ \mathrm{e}^{-mz/\bar{\gamma}}\ \mathrm{d}z. \tag{8}$$

Employing [21, §3.382, no. 4], one obtains

$$I_0 = 1\ -\ \frac{\Gamma(m, m\rho_0(\gamma_J+1)/\bar{\gamma})}{\Gamma(m)}, \tag{9}$$

where

$$\Gamma(a, x) = \int_x^\infty \xi^{a-1}\ \mathrm{e}^{-\xi}\ \mathrm{d}\xi \tag{10}$$

denotes the incomplete Gamma function [21, §8.350, no. 2].

The PDF $p(\gamma_J)$ of γ_J is of the same form as (5), where γ is to be replaced by γ_J, parameter m by m_J, and $\bar{\gamma}$ by $\bar{\gamma}_J := \mathrm{E}\{\gamma_J\}$.

Combining (4) and (9) along with the expression for $p(\gamma_J)$, one obtains

$$P_{BLEP,\rho_0} = 1 - \frac{m_J^{m_J}}{\bar{\gamma}_J^{m_J}\Gamma(m_J)\Gamma(m)} \times \\ \times \underbrace{\int_0^\infty \gamma_J^{m_J-1}\ \mathrm{e}^{-m_J\gamma_J/\bar{\gamma}_J}\ \Gamma(m, m\rho_0(\gamma_J+1)/\bar{\gamma})\ \mathrm{d}\gamma_J}_{=:I_1}. \tag{11}$$

Unfortunately, to the best of knowledge there is no closed-form solution for integral I_1, mainly due to the complicated argument of the incomplete gamma function. Yet, following [11], the analysis can be restricted to the special case of integer-valued Nakagami fading parameters $m \geq 1$, which covers many cases of practical interest (namely Rayleigh fading and lighter fading conditions). In this case, we can invoke [21, §8.352, no. 4]

$$\Gamma(n, x) = (n-1)!\ \mathrm{e}^{-x} \sum_{i=0}^{n-1} \frac{x^i}{i!} \quad (n = 1, 2, \ldots), \tag{12}$$

which leads to the following integral:

$$I_1 = \mathrm{e}^{-m\rho_0/\bar{\gamma}} \int_0^\infty \mathrm{e}^{-\zeta\gamma_J}\ \gamma_J^{m_J-1} \times \\ \times \sum_{i=0}^{m-1} \left(\frac{m\rho_0}{\bar{\gamma}}\right)^i \frac{1}{i!}\ (\gamma_J+1)^i\ \mathrm{d}\gamma_J, \tag{13}$$

where

$$\zeta := \frac{m\rho_0}{\bar{\gamma}} + \frac{m_J}{\bar{\gamma}_J}. \tag{14}$$

Moreover, we have employed the identity $\Gamma(n) = (n-1)!$ for integer values of n. Invoking the binomial theorem [21, §1.111]

$$(a+x)^n = \sum_{k=0}^{n} \binom{n}{k} x^k\ a^{n-k} \quad (n = 1, 2, \ldots), \tag{15}$$

Integral I_1 can be further rewritten as

$$I_1 = \mathrm{e}^{-m\rho_0/\bar{\gamma}} \sum_{i=0}^{m-1} \left(\frac{m\rho_0}{\bar{\gamma}}\right)^i \sum_{k=0}^{i} \frac{1}{k!(i-k)!} \times \\ \times \int_0^\infty \mathrm{e}^{-\zeta\gamma_J}\ \gamma_J^{m_J+i-k-1}\ \mathrm{d}\gamma_J. \tag{16}$$

Based on [21, §3.351, no. 3], and restricting Nakagami fading parameter m_J to integer values ≥ 1, we thus arrive at the solution

$$I_1 = \mathrm{e}^{-m\rho_0/\bar{\gamma}} \sum_{i=0}^{m-1} \left(\frac{m\rho_0}{\bar{\gamma}}\right)^i \sum_{k=0}^{i} \frac{1}{k!(i-k)!} \times \times \frac{(m_j + i - k - 1)!}{\zeta^{m_J+i-k}}. \quad (17)$$

Combining (17) with (11), we obtain our final closed-form expression for the resulting BLEP of the desired link as a function of threshold parameter ρ_0 for integer-valued Nakagami fading parameters $m, m_J \geq 1$ and arbitrary average SNRs/ JNRs $\bar{\gamma}, \bar{\gamma}_J > 0$:

$$P_{BLEP,\rho_0} = 1 - \left(\frac{m_J}{\bar{\gamma}_J}\right)^{m_J} \mathrm{e}^{-m\rho_0/\bar{\gamma}} \times \sum_{i=0}^{m-1} \sum_{k=0}^{i} \frac{\phi_{i,k} \cdot \left(\frac{m\rho_0}{\bar{\gamma}}\right)^i}{\left(\frac{m\rho_0}{\bar{\gamma}} + \frac{m_J}{\bar{\gamma}_J}\right)^{m_J+i-k}} =: 1 - \Psi(\rho_0), \quad (18)$$

where

$$\phi_{i,k} := \frac{(m_J)_{i-k}}{k!(i-k)!}, \quad (19)$$

and

$$(a)_n := a \cdot (a+1) \cdots (a+n-1) \quad (20)$$

denotes the Pochhammer symbol.

3.1 | Asymptotic BLEP analysis

Inspecting (18), it can readily be seen that the term $\Psi(\rho_0)$ tends to zero when the average JNR $\bar{\gamma}_J$ tends to infinity. In other words, the resulting BLEP for the desired link tends to one. In particular, the term $\Psi(\rho_0)$ is asymptotically ($\bar{\gamma}_J \to \infty$) equal to

$$\Psi(\rho_0) \doteq m_J^{m_J} \mathrm{e}^{-m\rho_0/\bar{\gamma}} \times \sum_{i=0}^{m-1} \sum_{k=0}^{i} \phi_{i,k} \left(\frac{m\rho_0}{\bar{\gamma}}\right)^{k-m_J} \left(\frac{1}{\bar{\gamma}_J}\right)^{m_J}. \quad (21)$$

Correspondingly, the approach $\Psi(\rho_0) \to 0$ for $\bar{\gamma}_J \to \infty$ is faster with growing values of Nakagami fading parameter m_J, that is, for cases where the jamming link is characterized by particularly light signal fading. Yet, numerical evaluation of (18) presented in the following section shows that this effect is rather less significant, so that the average JNR $\bar{\gamma}_J$ turns out to be the key parameter for successful (from the jammer's perspective) corruption of the desired link.

3.2 | Analysis of capacity outage probability

Based on (18), we can also obtain a corresponding expression for the outage probability regarding the instantaneous channel capacity of the desired link T → R. Let

$$C_\mathrm{d} := B \cdot \log_2(1+\rho) \ \ \mathrm{bit/s} \quad (22)$$

denote the instantaneous channel capacity of the desired link as a function of the SINR ρ. The capacity outage probability is then given by

$$P_{\mathrm{C,d,out}} := \Pr\{C_\mathrm{d} \leq C_{\mathrm{d},0}\} = C(C_{\mathrm{d},0}), \quad (23)$$

where $C_{\mathrm{d},0}$ denotes the minimum acceptable instantaneous capacity, defined by the underlying user application(s). From (18), we can obtain a closed-form expression for the CDF $C(C_{\mathrm{d},0})$, by simply replacing variable ρ_0 by $2^{C_{\mathrm{d},0}/B} - 1$. Correspondingly, the capacity outage probability is given by

$$P_{\mathrm{C,d,out}} := 1 - \Psi\left(2^{C_{\mathrm{d},0}/B} - 1\right). \quad (24)$$

To the best of knowledge, this closed-form expression is new. So far, only the PDF $p(C_\mathrm{d})$ of the instantaneous capacity of the desired link has been derived for the considered scenario, which is found in [19]. Furthermore, the PDF expression in [19] applies only for the special case of a strong jammer/ interferer ($P_J\,|h_J|^2 \gg \sigma^2$, that is, $\rho \approx \gamma/\gamma_J$), whereas (24) is valid for arbitrary jamming scenarios.

4 | NUMERICAL PERFORMANCE EXAMPLES

In the following, numerical results are presented for the BLEP resulting for the desired link for various fading scenarios. In particular, focus will be on the interplay between the two Nakagami-fading parameters m and m_J and between the corresponding average link SNRs/JNRs $\bar{\gamma}$ and $\bar{\gamma}_J$.

Figure 2 shows numerical results for the BLEP P_{BLEP,ρ_0} for different combinations of Nakagami-fading parameters m, m_J. As an example, average link SNRs/JNRs of $\bar{\gamma} = 20$ dB and $\bar{\gamma}_J = 10$ dB are considered. Dashed lines represent Monte-Carlo simulation results, while the markers ∘ represent corresponding analytical results based on (18), which are in good accordance. As can be seen, low BLEP values for the desired link are only attained, when the required SINR ρ_0 is rather low and the Nakagami fading parameter for the desired link is significantly larger than for the jamming link (e.g. $m = 10$, $m_J = 1$). Otherwise the jammer will be able to significantly corrupt the desired link, even though there is an SNR advantage of 10 dB for the desired link in this example.

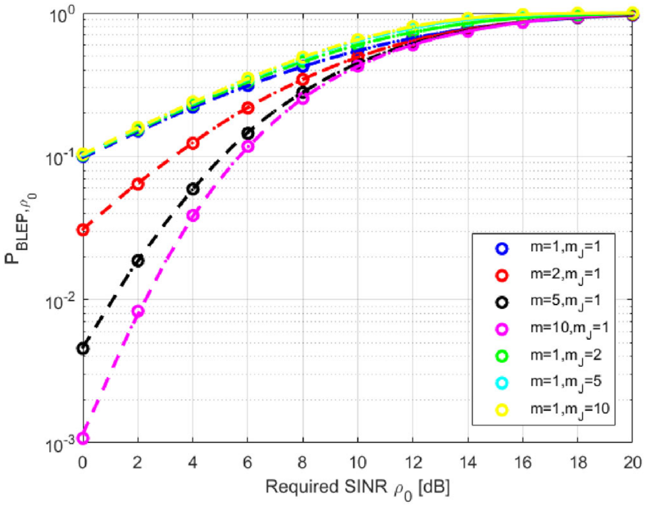

FIGURE 2 BLEP for the desired link as a function of the required SINR ρ_0 for different combinations of Nakagami-fading parameters m, m_J ($\bar{\gamma} = 20$ dB, $\bar{\gamma}_J = 10$ dB). Dashed lines: Monte-Carlo simulation results, markers ∘: analytical results based on (18).

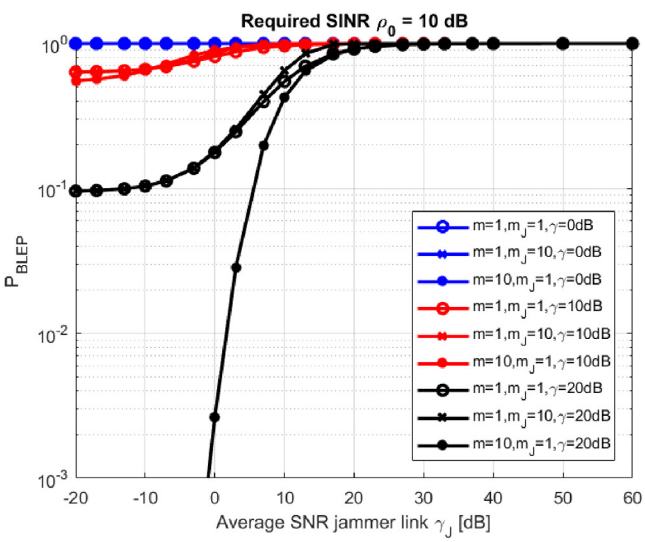

FIGURE 3 BLEP for the desired link as a function of the average JNR $\bar{\gamma}_J$ for different combinations of Nakagami-fading parameters m, m_J and different average SNRs $\bar{\gamma}$ of the desired link (required SINR $\rho_0 = 10$ dB); analytical results based on (18).

Figure 3 illustrates the asymptotic behavior of P_{BLEP,ρ_0} for large average JNRs $\bar{\gamma}_J$ discussed earlier based on the analytical results in Section 3. Obviously, P_{BLEP,ρ_0} tends to one for large average JNRs $\bar{\gamma}_J$, while the approach $P_{BLEP,\rho_0} \to 1$ for $\bar{\gamma}_J \to \infty$ is faster with growing values of Nakagami fading parameter m_J, as can for example be seen from the black curves associated with an average SNR of the desired link of $\bar{\gamma} = 20$ dB. However, this effect is rather less significant, so that the average JNR $\bar{\gamma}_J$ turns out to be the key parameter for successful corruption of the desired link.

An overview regarding the interplay between the Nakagami-fading parameters m and m_J and the average link SNRs/ JNRs

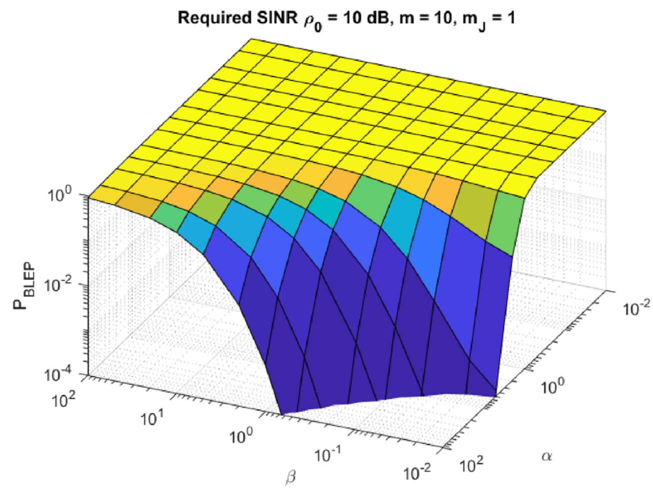

FIGURE 4 BLEP for the desired link as a function of the average link SNR/JNR $\bar{\gamma} := \alpha\,\rho_0$ and $\bar{\gamma}_J := \beta\,\rho_0$ related to the required SINR ρ_0; Nakagami-fading parameters $m = 10$, $m_J = 1$ ($\rho_0 = 10$ dB); analytical results based on (18).

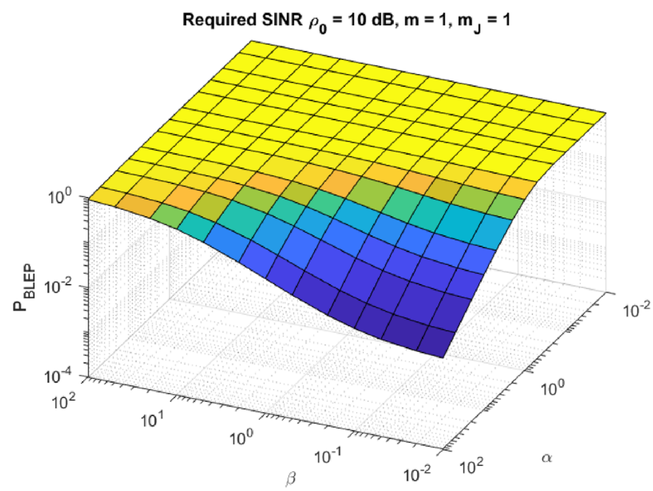

FIGURE 5 BLEP for the desired link as a function of the average link SNR/JNR $\bar{\gamma} := \alpha\,\rho_0$ and $\bar{\gamma}_J := \beta\,\rho_0$ related to the required SINR ρ_0; Nakagami-fading parameters $m = 1$, $m_J = 1$ ($\rho_0 = 10$ dB); analytical results based on (18).

$\bar{\gamma}$ and $\bar{\gamma}_J$ can be gained from the three-dimensional plots in Figures 4–6. Here, $\bar{\gamma}$ and $\bar{\gamma}_J$ are related to the required SINR ρ_0 at the desired receiver according to $\bar{\gamma} := \alpha\,\rho_0$ and $\bar{\gamma}_J := \beta\,\rho_0$. As can be seen, when the desired link is characterized by significantly lighter fading than the jamming link (Figure 4), there is a region where low BLEP values are attained for the desired link, associated with low values of the average JNR $\bar{\gamma}_J$ ($\beta < 1$) and high values of the average SNR $\bar{\gamma}$ of the desired link ($\alpha > 1$). However, when both links are characterized by more severe fading (in this example, by Rayleigh fading $m = m_J = 1$), the region of low BLEP values disappears for the considered values of α and β (Figure 5). When instead the jamming link is characterized by significantly lighter fading than the desired link (Figure 6), the additional effect is rather minor, although the "waterfall"

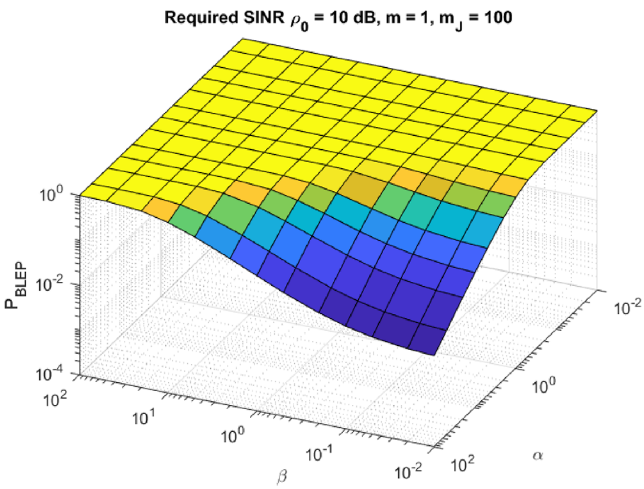

FIGURE 6 BLEP for the desired link as a function of the average link SNR/JNR $\bar{\gamma} := \alpha\,\rho_0$ and $\bar{\gamma}_J := \beta\,\rho_0$ related to the required SINR ρ_0; Nakagami-fading parameters $m = 1$, $m_J = 100$ ($\rho_0 = 10$ dB); analytical results based on (18).

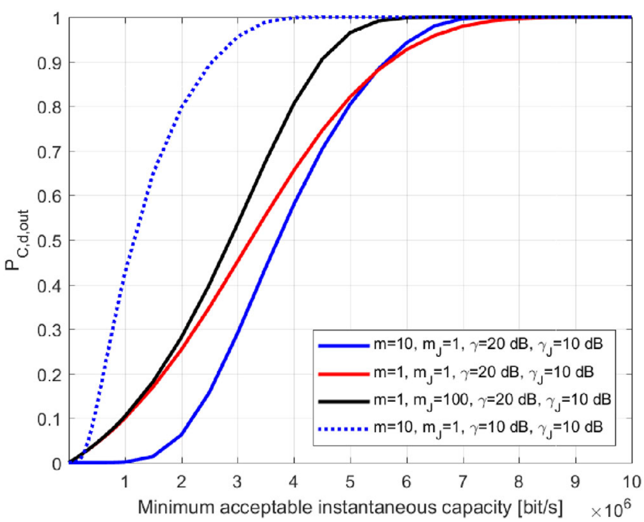

FIGURE 7 Capacity outage probability for the desired link as a function of the minimum acceptable instantaneous channel capacity for different combinations of Nakagami-fading parameters m, m_J and average SNRs/ JNRs $\bar{\gamma}, \bar{\gamma}_J$ ($B = 1$ MHz); analytical results based on (24).

region of the BLEP is pushed slightly further in the direction of $\beta = 10^{-2}$ and $\alpha = 10^2$ in this example.

Numerical results regarding the capacity outage probability $P_{\mathrm{C,d,out}}$ (24) for different combinations of Nakagami-fading parameters m, m_J and average SNRs/ JNRs $\bar{\gamma}$, $\bar{\gamma}_J$ are presented in Figure 7, where an exemplary frequency bandwidth of 1 MHz was chosen. As expected, the capacity outage probability exhibits a similar behavior as discussed earlier for the BLEP. As long as the desired link has a significant SNR advantage ($\bar{\gamma} \gg \bar{\gamma}_J$) and significantly better fading conditions ($m \gg m_J$), favorable instantaneous channel capacities are obtained with high probability (that is, with an outage probability close to zero), which are basically in accordance with the employed bandwidth B. However, when the fading conditions for the jammer link are similar or even better than for the desired link, a significant performance degradation is observed. Yet, the key parameter is given by the average JNR. If the jamming link has a significant SNR advantage ($\bar{\gamma} \ll \bar{\gamma}_J$), the instantaneous capacity values obtained for the desired link are drastically reduced, even if the desired link has significantly better fading conditions ($m \gg m_J$). In fact, this deterioration already starts for equal SNR/ JNR conditions on both links ($\bar{\gamma} = \bar{\gamma}_J$), as can be seen in Figure 7.

5 | EXTENSIONS TO MULTIPLE-ANTENNA SETTINGS

So far, focus has been on scenarios where all nodes (T, R, and J) employ a single antenna. In the following, we discuss corresponding extensions of our presented analyses regarding array processing and diversity reception.

5.1 | Array processing

If the jammer J employs an antenna array consisting of M_J transmit antenna elements, it can form a directive antenna pattern by applying (analog or digital) phase shifts to the individual antenna branches [22]. Provided that the jammer knows (or has learned) the direction of the desired receiver R, a corresponding beamforming gain in direction of R can be generated by this means. Theoretically, the maximum beamforming gain is given by M_J, which will be reduced by a factor $\delta_J \leq 1$ in practice, due to jammer hardware non-idealities and noisy estimates regarding the exact direction of R. As a result, the average JNR of the jamming link J → R will be given by $\bar{\gamma}'_J = \delta_J M_J \bar{\gamma}_J$, where $\bar{\gamma}_J$ denotes the average JNR in the single-antenna case, cf. Section 3. Thus, the transmit antenna array of the jammer transforms the jamming link J → R into an equivalent single-antenna link with an increased average JNR.

Similarly, if the transmitter T employs an antenna array consisting of M transmit antenna elements, it can transform the desired link T → R into an equivalent single-antenna link with an average SNR increased by a factor of $\delta_T M$ ($\delta_T \leq 1$). On the other hand, if the desired receiver R employs an antenna array consisting of N receive antenna elements, it can place a minimum within the receive antenna pattern in direction of the jammer J. However, due to noise and a finite width of the attained minimum (in combination with non-perfect estimates regarding the jammer's direction), an exact nulling of the jamming signal will not be possible in practice. Therefore, we define a power attenuation factor $\epsilon_R \geq 0$ for the direction of the jammer J relative to the direction of the desired transmitter T. Note that ϵ_R tends to decrease with an increasing number N of receive antenna elements. As a result, the average JNR of the jamming link J → R will be given by $\bar{\gamma}''_J = \epsilon_R\, \delta_J\, M_J\, \bar{\gamma}_J$.

Based on the above considerations, we may reuse our BLEP expression (18) by replacing $\bar{\gamma}_J$ with $\bar{\gamma}''_J$ (or $\bar{\gamma}'_J$). Depending on the hardware conditions of the jammer and the desired receiver, the quality of direction estimates, and the number of antenna elements M_J, N, the BLEP performance of the desired link

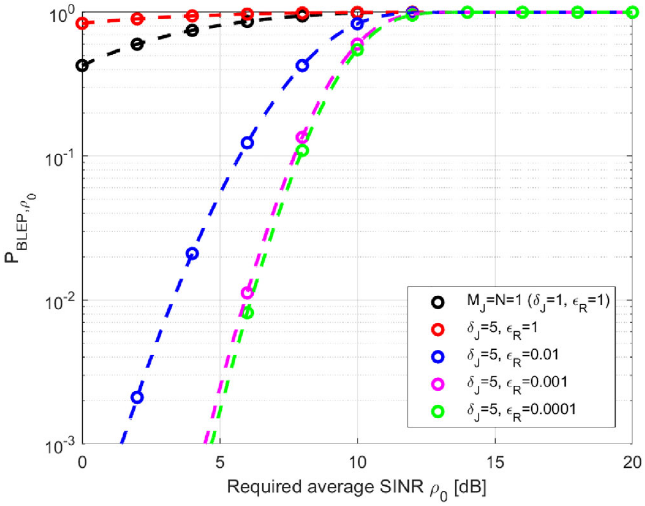

FIGURE 8 BLEP for the desired link as a function of the required SINR ρ_0 for the case of array processing with different combinations of the parameters δ_J and ϵ_R ($\delta_T = 1$, $m = 10$, $m_J = 1$, $\bar{\gamma} = \bar{\gamma}_J = 10$ dB). Dashed lines: Monte-Carlo simulation results, markers ∘: analytical results based on (18).

will either improve ($\epsilon_R \delta_J M_J < 1$) or deteriorate ($\epsilon_R \delta_J M_J > 1$). Figure 8 shows corresponding BLEP results for the case $\delta_T = 1$, $m = 10$, $m_J = 1$, equal average link SNRs/ JNRs of $\bar{\gamma} = \bar{\gamma}_J = 10$ dB, and different combinations of δ_J and ϵ_R. As can be seen, transmit beamforming at the jammer J further degrades the BLEP performance of the desired link, if it is not countered by corresponding array processing at the receiver R (red curve, $\epsilon_R = 1$). On the other hand, if the jamming link is suppressed by means of array processing at the receiver R, the BLEP performance of the desired link can be improved significantly. However, the attainable performance is limited by the fading parameter m of the desired link, which becomes obvious from the marginal BLEP improvement when decreasing the factor ϵ_R from 0.001 to 0.0001. In other words, array processing at the receiver R does not require any SNR advantage of the desired link compared to the jamming link, but still suffers from non-favorable fading conditions on the desired link (represented by small values of m).

5.2 | Diversity reception

Regarding array processing, typical antenna spacings are on the order of $\lambda/2$, where λ denotes the carrier wavelength of the desired and the jamming signals. As an alternative to receive array processing, the performance of the desired link T → R may also be improved by utilizing multiple receive antennas with spacing $> \lambda/2$ at the desired receiver in conjunction with MRC. To this end, the N receive branches are weighted by the complex-conjugates of the channel coefficients h_i associated with the desired links from transmitting node T to the individual receive antennas ($1 \le i \le N$) and are then linearly combined. In particular, the receive antenna spacing is chosen sufficiently large, such that the channel coefficients h_i may be regarded as statistically independent. For the desired signal, this leads to a constructive superposition ($\gamma \propto \sum_{i=1}^{N} |h_i|^2$), whereas noise and jamming/ interfering signals are combined incoherently, giving rise to a corresponding diversity gain [23]. Note that explicit estimation of the jammer's direction is not required for diversity reception. Assuming an identical fading parameter m for all channel coefficients h_i, the PDF of the instantaneous desired link SNR γ after MRC can be shown to be [7]

$$p(\gamma) = \frac{m^{mN} \gamma^{mN-1}}{\bar{\gamma}^{mN} \Gamma(mN)} \, \mathrm{e}^{-m\gamma/\bar{\gamma}}. \tag{25}$$

Correspondingly, the general form of $p(\gamma)$ remains the same as in the single-antenna case (cf. (5)), as diversity reception transforms the desired link T → R into an equivalent single-antenna link with increased fading parameter mN (and therefore more favorable fading conditions). The same rationale also holds for M transmit and N receive antenna elements in conjunction with space-time coding [24], where the effective fading parameter results as mMN.

Regarding the jamming link J → R, a common assumption in the literature is that the jamming/ interfering signal is the same for all receive branches, even if multipath fading is assumed for the jamming link [7, 11]. Yet, if antenna spacings are chosen large enough to provide uncorrelated channel coefficients h_i for the desired link T → R—and since the jammer and the desired link operate in the same frequency band—it seems reasonable to assume the same for the channel coefficients $h_{J,i}$ of the jamming link J → R (rather than assuming fully correlated channel coefficients $h_{J,1} = \cdots = h_{J,N}$). Due the MRC step, the instantaneous JNR is of form

$$\gamma_J \propto \frac{\left|\sum_{i=1}^{N} h_i^* h_{J,i}\right|^2}{\sum_{i=1}^{N} |h_i|^2} \tag{26}$$

with uncorrelated channel coefficients $h_{J,i}$. Unfortunately, a closed-form expression of the PDF of γ_J seems difficult to obtain for the considered case of Nakagami-m/m_J fading, which hinders a more detailed analysis of the resulting SINR ρ and the corresponding BLEP. In the following, we therefore resort to Monte-Carlo computer simulations, in order to assess the effect of diversity reception.

Figure 9 shows corresponding BLEP results for the case $m = 1$, $m_J = 5$, average link SNRs/ JNRs of $\bar{\gamma} = 20$ dB and $\bar{\gamma}_J = 10$ dB, and different numbers N of diversity branches. The BLEP curves represented by solid lines were obtained based on the expression (26) for the instantaneous JNR γ_J, whereas the dashed lines resulted for the simplified assumption that the jamming/ interfering signal is the same for all receive branches. As can be seen, there is a notable difference between the two models. Furthermore, diversity reception can significantly improve the BLEP performance of the desired link in this examples. Further simulations not included here for the sake of conciseness show that the attainable performance is limited by the average SNR $\bar{\gamma}$ of the desired link, however. In other words,

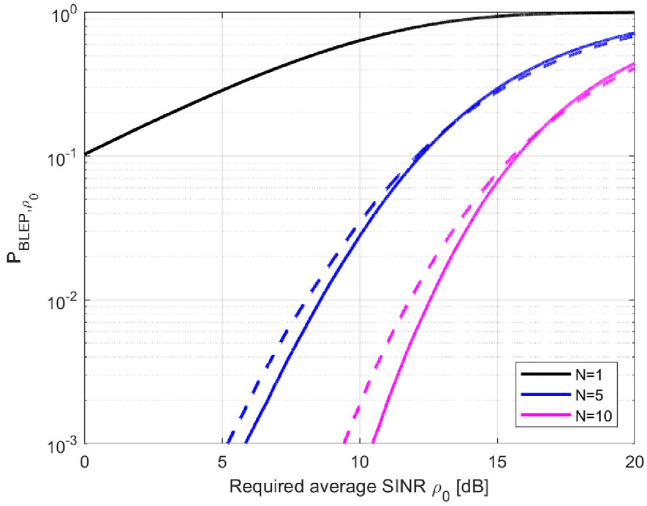

FIGURE 9 BLEP for the desired link as a function of the required SINR ρ_0 for the case of diversity reception for different numbers of receive antennas N ($m = 1$, $m_J = 5$, $\bar{\gamma} = 20$ dB, $\bar{\gamma}_J = 10$ dB, Monte-Carlo simulation results).

diversity reception does not require any advantage of the desired link regarding the fading conditions compared to the jamming link, but still suffers from non-favorable SNR conditions on the desired link (represented by small values of $\bar{\gamma}$). Therefore, it somewhat complements the option of receive array processing discussed above.

6 | CONCLUSIONS

We have derived a simple closed-form analytical expression for the BLEP of a wireless link in the presence of a jamming link, when both links are subject to Nakagami-*m* fading with in general different average SNRs/ JNRs and integer-valued fading parameters. An asymptotic expression for high average JNRs has also been devised. As a result, the BLEP tends to one when the average JNR tends to infinity. Moreover, the effect of the Nakagami fading parameter of the jamming link was found to be rather less significant, so that the average JNR turned out to be the key parameter for successful corruption of the desired link. As a bottom line, in the single-antenna case the jammer will be able to successfully corrupt the desired link, unless there is a rather high SNR advantage for the desired link—even if the jamming link is characterized by a significantly smaller Nakagami fading parameter (i.e. more severe multipath signal fading) than the desired link. From a system design point of view under multipath signal fading, this means that single-antenna links employing static frequency bands can only counter jamming by drastically increasing their transmit power.

Utilizing multiple antennas at the desired receiver—paired with suitable beamforming algorithms for adaptive nulling of the jammer or corresponding diversity reception schemes—has been found to be a promising solution to counter jamming. In particular, it was shown that receive array processing at the desired receiver can significantly improve the resulting BLEP, provided that the desired link is characterized by rather favorable fading conditions—even if the desired and the jamming link are characterized by similar SNR/ JNR conditions. On the other hand, diversity reception at the desired receiver can significantly improve the resulting BLEP, provided that the desired link is characterized by favorable SNR conditions—even if the jamming link has more favorable fading conditions.

If the desired link is neither characterized by favorable fading conditions nor by favorable SNR conditions, alternative or complementary solutions are required, however. One option is to employ a quasi-random frequency hopping scheme for the desired link. Yet, this may be countered by employing *responsive jamming* rather than barrage jamming [25]. Another innovative solution is that the desired transmitter may also utilize the jamming signal itself by back-scattering modulated information on the jamming signal [26]. To this end, the behavior of the jammer needs to be learned by the desired transmitter, which may be attained by means of suitable machine-learning techniques (e.g., reinforcement learning).

For future work, it would be interesting to study cases of more severe signal fading, including long-term fading and shadowing effects, by looking at more general fading models (e.g. [27]).

AUTHOR CONTRIBUTIONS

Jan Mietzner: Conceptualization; formal analysis; investigation; methodology; project administration; software; validation; visualization; writing (original draft preparation and review & editing).

ACKNOWLEDGEMENTS

Many thanks to Dr. Ronald Boehnke (Huawei Technologies Duesseldorf GmbH, Munich Research Center) for fruitful discussions regarding some details of the presented derivations. The author acknowledges support for the article processing charge by the Open Access Publication Fund of Hamburg University of Applied Sciences.

CONFLICT OF INTEREST STATEMENT

The authors declare no conflicts of interest

DATA AVAILABILITY STATEMENT

Data available on request from the authors.

ORCID

Jan Mietzner https://orcid.org/0000-0001-9084-9443

REFERENCES

1. Shafi, M., Molisch, A.F., Smith, P.J., Haustein, T., Zhu, P., Silva, P.D., Tufvesson, F., Benjebbour, A., Wunder, G.: 5G: A tutorial overview of standards, trials, challenges, deployment, and practice. IEEE J. Sel. Areas Commun. 35(6), 1201–1221 (2017)
2. Abu-Dayya, A.A., Beaulieu, N.C.: Diversity MPSK receivers in cochannel interference. IEEE Trans. Veh. Technol. 48(6), 1959–1965 (1999)
3. McKay, M.R., Zanella, A., Collings, I.B., Chiani, M.: Error probability and SINR analysis of optimum combining in Rician fading. IEEE Trans. Commun. 57(3), 676–687 (2009)
4. Belmekki, B.E.Y., Hamza, A., Escrig, B.: On the outage probability of vehicular communications at intersections over Nakagami-*m* fading

channels. In: Proceedings of IEEE 91st Vehicular Technology Conference (VTC-Spring). IEEE, Piscataway (2020)
5. Villier, E.: Performance analysis of optimum combining with multiple interferers in flat Rayleigh fading. IEEE Trans. Commun. 47(10), 1503–1510 (1999)
6. Sagias, N.C.: Closed-form analysis of equal-gain diversity in wireless radio networks. IEEE Trans. Veh. Technol. 56(1), 173–182 (2007)
7. Aalo, V., Zhang, J.: Performance analysis of maximal ratio combining in the presence of multiple equal-power cochannel interferers in a Nakagami fading channel. IEEE Trans. Veh. Technol. 50(2), 497–503 (2001)
8. da Costa, D.B., Yacoub, M.D.: Outage performance of two hop AF relaying systems with co-channel interferers over Nakagami-m fading. IEEE Commun. Lett. 15(9), 980–982 (2011)
9. Ermolova, N.Y., Tirkkonen, O.: Outage probability analysis in generalized fading channels with co-channel interference and background noise: $\eta-\mu/\eta-\mu$, $\eta-\mu/\kappa-\mu$, and $\kappa-\mu/\eta-\mu$ scenarios. IEEE Trans. Wireless Commun. 13(1), 291–297 (2014)
10. Zhang, Q.T.: Outage probability in cellular mobile radio due to Nakagami signal and interferers with arbitrary parameters. IEEE Trans. Veh. Technol. 45(2), 364–372 (1996)
11. Romero-Jerez, J.M., Pe na Martín, J.P., Goldsmith, A.J.: Outage probability of MRC with arbitrary power cochannel interferers in Nakagami fading. IEEE Trans. Commun. 55(7), 1283–1286 (2007)
12. Rached, N.B., Kammoun, A., Alouini, M.-S., Tempone, R.: A unified moment-based approach for the evaluation of the outage probability with noise and interference. IEEE Trans. Wireless Commun. 16(2), 1012–1023 (2017)
13. Akhlaghpasand, H., Björnson, E., Razavizadeh, S.M.: Jamming suppression in massive MIMO systems. IEEE Trans. Circ. Syst. II: Exp. Briefs 67(1), 182–186 (2020)
14. Bagherinejad, S., Razavizadeh, S.M.: Direction-based jamming detection and suppression in mmWave massive MIMO networks. IET Communications 15(14), 1780–1790 (2021)
15. Zheng, T.-X., Yang, Z., Wang, C., Li, Z., Yuan, J., Guan, X.: Wireless covert communications aided by distributed cooperative jamming over slow fading channels. IEEE Trans. Wireless Commun. 20(11), 7026–7039 (2021)
16. Chen, B., Li, R., Ning, Q., Lin, K., Han, C., Leung, V.: Security at physical layer in NOMA relaying networks With cooperative jamming. IEEE Trans. Veh. Technol. 71(4), 3883–3888 (2022)
17. Allipuram, S., Mohapatra, P., Pappas, N., Parmar, S., Chakrabarti, S.: Performance analysis of a MIMO system With bursty traffic in the presence of energy harvesting jammer. IEEE Trans. Green Commun. and Networking 6(2), 1157–1172 (2022)
18. Huang, H., Zhang, Y., Zhang, H., Cai, Y., Swindlehurst, A.L., Han, Z.: Disco intelligent reflecting surfaces: active channel aging for fully-passive jamming attack. IEEE Trans. Wireless Commun. 23(1), 806–819 (2024)
19. Yao, Y.D., Sheikh, A.U.H.: Evaluation of channel capacity in a generalized fading channel. In: Proceedings of IEEE 43rd Vehicular Technology Conference, pp. 134–137. IEEE, Piscataway (1993)
20. Nakagami, M.: The m distribution: A general formula for intensity distribution of rapid fading. In: W. C. Hoffman (ed.) Statistical Methods in Radio Wave Propagation. Pergamon, New York (1960)
21. Gradsheteyn, I.S., Ryzhik, I.M.: Table of Integrals, Series, and Products. 7th edn. Academic Press, New York (1994)
22. Krim, H., Viberg, M.: Two decades of array signal processing research: the parametric approach. IEEE Signal Proc. Mag. 13(4), 67–94 (1996)
23. Mietzner, J., Schober, R., Lampe, L., Gerstacker, W.H., Hoeher, P.A.: Multiple-antenna techniques for wireless communications - A comprehensive literature survey. IEEE Commun. Surv. Tutor. 11(2), 87–105 (2009)
24. Alamouti, S.: A simple transmit diversity technique for wireless communications. IEEE J. Sel. Areas Commun. 16(8), 1451–1458 (1998)
25. Mietzner, J., Nickel, P., Meusling, A., Loos, P., Bauch, G.: Responsive communications jamming against radio-controlled improvised explosive devices. IEEE Commun. Mag. 50(10), 38–46 (2012)
26. Huynh, N.V., Nguyen, D.N., Hoang, D.T., Dutkiewicz, E.: Jam me if you can: Defeating jammer with deep dueling neural network architecture and ambient backscattering augmented communications. IEEE J. Sel. Areas Commun. 37(11), 2603–2620 (2019)
27. Zhu, C., Mietzner, J., and Schober, R.: On the performance of non-coherent transmission schemes with equal-gain combining in generalized K-fading. IEEE Trans. Wireless Commun. 9(4), 1337–1349 (2010)

How to cite this article: Mietzner, J.: Analysis of error rates and capacity outage of wireless links under jamming and multipath signal fading. IET Commun. 1–10 (2024). https://doi.org/10.1049/cmu2.12858